

Z-99 TIME-LAPSE SHEAR WAVE SPLITTING ANALYSIS AT EKOFISK FIELD, NORTH SEA

R. VAN DOK¹, J. GAISER¹ and T. PROBERT²

¹WesternGeco, 1625 Broadway, Suite 1300, Denver, Colorado, 80202, USA

² WesternGeco, Schlumberger House, Buckingham Gate, Gatwick, UK

Summary

The ability to detect and measure shear-wave (S-wave) birefringence, or shear splitting, using mode-converted (PS) waves is well understood and is demonstrated in several recent studies. In September 2002, a 4-component (4C) test line was acquired at the Ekofisk Field to investigate the application of PS-waves. Analysis of the PS-wave data indicated the presence of significant S-wave birefringence in the near surface. This phenomenon has been correlated to the local sea floor subsidence that is induced by the compaction within the underlying chalk reservoir at a depth of approximately 3 km. A second 4C test line was acquired in December 2003 at the same location. Comparison of the two surveys allows the analysis of the changes in the observed S-wave splitting over this period.

Introduction

Use of S-wave splitting analysis has been gaining interest over the past several years and has been shown to be an important tool for investigating unequal horizontal stress fields and fracture characterization. Vetri et al. (2003) used P and PS-waves to characterize a fractured reservoir in the Adriatic Sea, and Olofsson et al. (2003) and Van Dok et al. (2003) used PS-waves to estimate seabed birefringence in the North Sea, which showed a possible correlation to shallow seabed subsidence. This may be particularly important for evaluating geomechanical properties and drilling hazards.

The purpose of this paper is to investigate time-lapse measurements of S-wave birefringence for the shallow seabed at the Ekofisk Field. Two 2D line surveys, acquired a year apart, both show the same near surface effects observed at the nearby Valhall Field. This time-lapse experiment will help our understanding of the changes over time of S-wave splitting attributes as well as any variations expected due to survey design geometry, sensor type or other geophysical property changes.

Background

Ekofisk Field was discovered in 1969 and has been producing since 1971. The reservoir is trapped within a large anticline structure consisting of a high porosity chalk. Approximately one third of the reservoir is seismically obscured on existing P-wave seismic data due to the presence of free gas and overpressured shales within the overburden.

In September 2002, a 2D/4C VectorSeis OBC test was acquired over the western edge of the seismically obscured area with half of the cable positioned over the gas cloud and half outside it. The cable itself consisted of 40 non-gimbaled 4C detectors utilizing a hydrophone and three orthogonal accelerometers spaced 50 m apart. A blanket of air gun sources was used to provide wide azimuth coverage over the detector locations, as shown in Figure 1. The source spacing was 25 m and the source-line spacing was approximately 100 m. In October 2003, a second survey was acquired with a Q-Seabed OBC in the nearly same location utilizing 160 non-gimbaled 4C sensors but at a spacing of 12.5 m. The source spacing was 50 m with a source-line spacing of 100 m.

Data Processing

Processing of both the P-wave and PS-wave data was primarily limited to a 2D test line extracted from the center of the survey over the top of the cable. The processing sequence for the P-wave data included vector fidelity analysis and compensation, hydrophone/geophone (PZ) summation,

deconvolution, residual statics, and pre-stack Kirchhoff time migration. The PS-wave data processing included vector fidelity analysis and compensation, horizontal geophone orientation analysis, rotation to radial and transverse components, long-period detector static corrections, deconvolution, CCP binning, PS-wave DMO and common-offset time migration.

Determination of Principal S-Wave Directions

In order to determine the principal directions of the S-waves (S1 and S2) common-azimuth stacks were created for each detector location using the 3D blanket of sources. For a given detector, 10-degree azimuth-bin stacks of both the radial and transverse components were created producing 72 stacked seismic traces. The data were NMO corrected and offset-limited to 500 meters before stacking. Azimuth-bin stacks for detector location 1 are shown in Figure 2. A key indication of the principal directions is the attenuation of the energy on the transverse component. Null traces occur on the transverse component when the source-to-detector azimuth aligns with either S1 or S2. To accurately measure the time delays between the fast and slow S-waves a 2Cx2C Alford rotation and layer-stripping algorithm was applied to the common-azimuth stacks. This method groups 36 radial and 36 transverse azimuth-bin stacks into orthogonal azimuths to produce the necessary 4C data for Alford rotation. For this study, a shallow analysis window (0-550 ms) was used in order to isolate and investigate the effects of S-wave birefringence in the near surface geology.

Time Lapse Processing and Analysis

In order to investigate the time-lapse effects of the S-wave splitting, the processing and analysis methods described above were repeated on the same 40 detector locations extracted from the 2003 survey. Ideally, all acquisition related differences are removed before any time-lapse analysis is performed. This includes differences in the acquisition design, the recording system (instrument and sensor responses), the source signature, noise levels, sea floor coupling and vector fidelity.

The resulting S1 orientations and percent anisotropy values for both surveys are shown in the graphs in Figures 3 and 4 along with the computed differences. The results indicate that a small change has occurred in both the direction and magnitude during the time interval between the two surveys.

Results

It is well known that differential stress fields can preferentially open fracture sets and pore spaces in the principal horizontal stress direction and cause S-waves to polarize and split. The amount of birefringence depends on the difference in the stress fields or the density of fractures (or micro fractures), assuming a uniformly fractured medium. The chalk reservoir at Ekofisk has compacted as a result of rapid pressure depletion during the early years of production and water weakening effects caused by the injection of seawater. This compaction process has caused the seabed to subside by over 8 meters since the beginning of production, leaving a large bowl-shaped depression on the sea floor. This subsidence can induce a stress field at the sea floor where the maximum horizontal stress would be parallel with contours of the depression and the magnitude of differential horizontal stress would be proportional to the change in slope. It is believed that the increased magnitude of S-wave birefringence is associated with increased differential stress along the edges of the subsidence zone and the orientation of the stress field is sub-parallel to the contours. It also indicates that the magnitude of the birefringence is decreasing towards the center, possibly due to a smaller differential stress field in this area. In general, the scatter in the orientation measurements is less than +/- 5 degrees and the percent anisotropy less than +/- 1%.

In addition, the change in the percent anisotropy observed over the one-year interval between surveys indicates that it may be possible to monitor local short-term changes in the near-surface stress field. Further study is needed into the possible causes of this variation in order to determine if these are in response to changes in the differential stress fields or differences in the acquisition. Note that the curves in Figures 3 and 4 are in good agreement where the detector locations are very close for the two surveys but differ slightly where the two lines diverge.

Conclusions

Changes in the observed shear-wave splitting were observed when comparing two 4C test surveys acquired over a one-year interval at the Ekofisk Field. The changes were in both the orientation of the

fast shear wave and the magnitude of the anisotropy. The scatter of the orientation was ± 5 degrees on average and $\pm 1\%$ for the anisotropy. An apparent change occurred over time along the center of the cable but this area corresponds to where detectors were not collocated. Further study into the possible origins of this change is necessary.

References

- Olofsson, B., Probert, T., Kommedal, J.H. and Barkved, O.I. 2003. Azimuthal anisotropy from the Valhall 4C 3D survey. *The Leading Edge*, **22**, 1228-1235.
- Van Dok, R.R., Gaiser, J.E., and Byerley, G. 2003. Near-surface shear-wave birefringence in the North Sea: Ekofisk 2D/4C test. *The Leading Edge*, **22**, 1236-1242.
- Vetri, L., Loinger, E., Gaiser, J.E., Grandi, A. and Lynn, H. 2003. 3D/4C Emilio: Azimuth processing and anisotropy analysis in a fractured carbonate reservoir. *The Leading Edge*, **22**, 675-679.

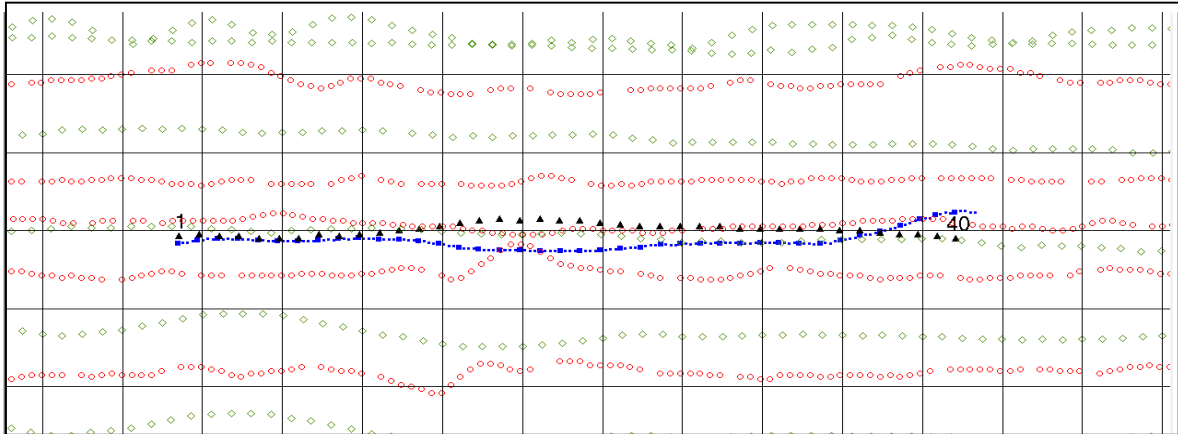


Figure 1. Map showing the source and detector locations for the 2002 survey (red source circles and black detector triangles) and the 2003 survey (green source diamonds and blue detector squares). Note that the 2002 survey used a 50 m detector spacing and 25 m source spacing while the 2003 used a 12.5 m detector spacing and 50 m source spacing. A blanket of sources (not all shown) was utilized providing wide azimuth coverage at each detector.

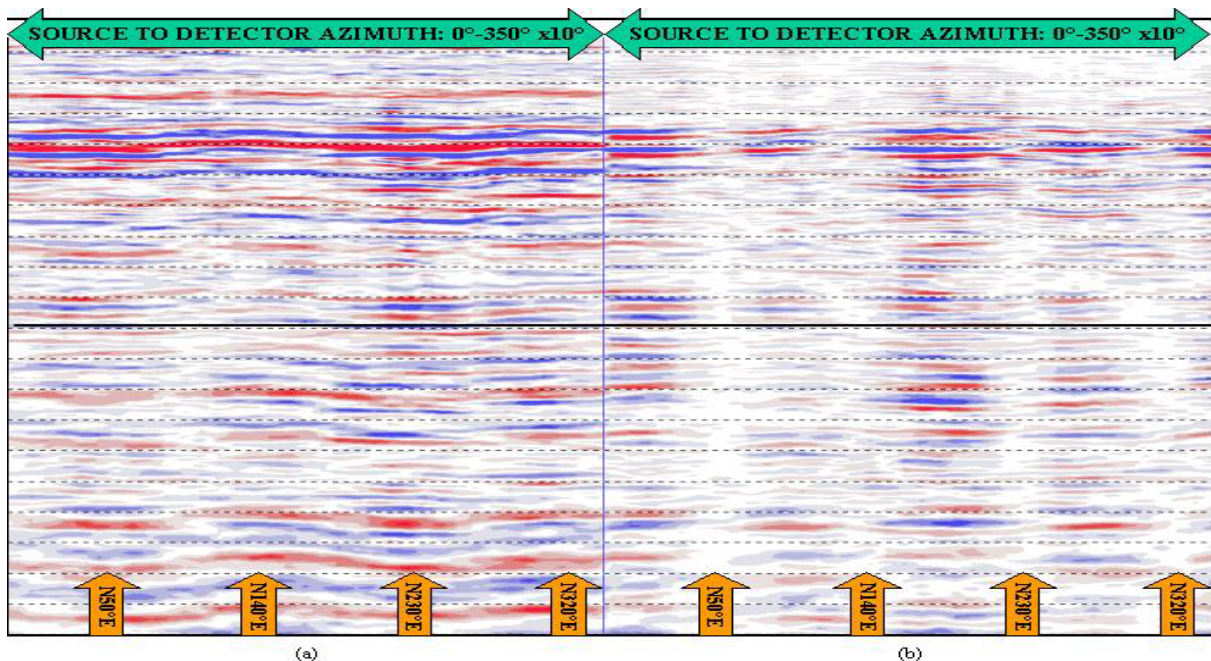


Figure 2. Azimuth-limited common-detector stack traces from detector location 1: a) radial and b) transverse component. Approximate principal S-wave directions at 50, 140, 230 and 320 degrees, as determined by locating the null transverse component traces, are shown as orange arrows. Note the polarity change across these null zones and that the directions are separated by 90 degrees.

Fast S-wave (S1) Orientation

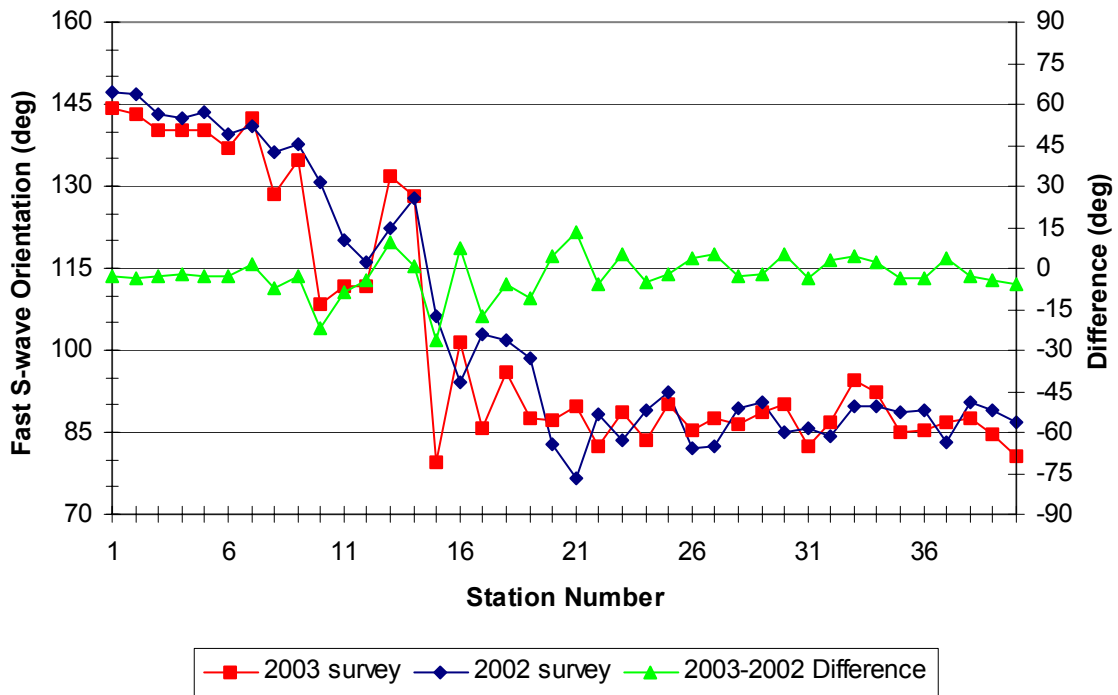


Figure 3. Graph showing the S1 orientation determined from the 2002 and 2003 surveys. The green curve shows the difference in S1 orientation between the two surveys.

S-wave % Anisotropy

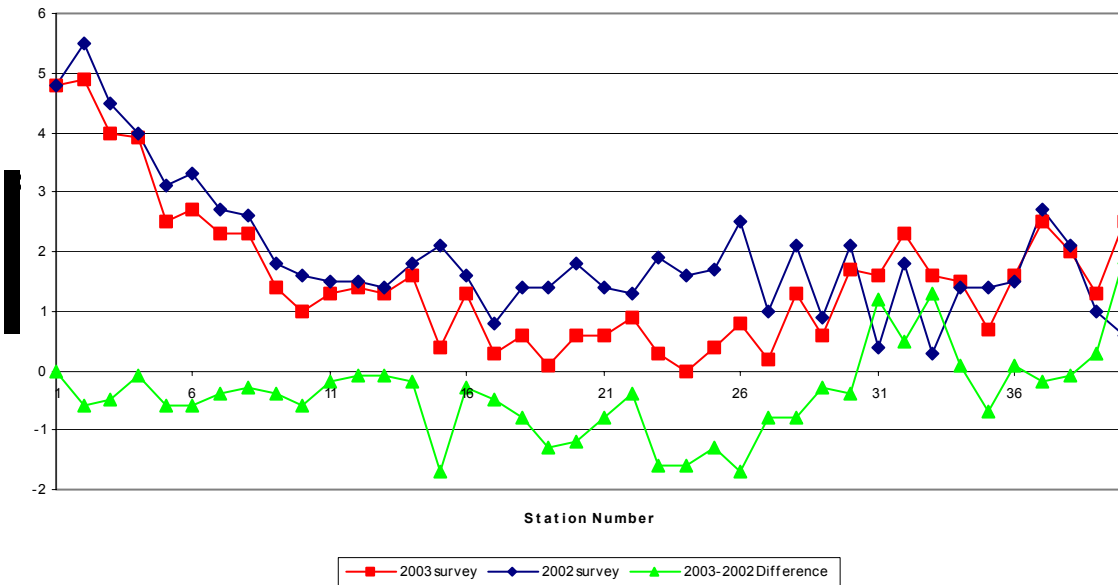


Figure 4. Graph showing the percent anisotropy determined from the 2002 and 2003 surveys. The green curve shows the difference in the percent anisotropy with time. A general decrease is observed over time for the western portion of the line.